Pergamon

Geochimica et Cosmochimica Acta, Vol. 68, No. 20, pp. 4179-4188, 2004

0016-7037/04 $30.00 + .00

doi:10.1016/j.gca.2004.02.024

Experimental determination of Ni diffusion coefficients in olivine and their dependence on temperature, composition, oxygen fugacity, and crystallographic orientation

CHRISTOF PETRY,[1] SUMIT CHAKRABORTY,[2,*] and HERBERT PALME[1]

[1]Institut für Mineralogie und Geochemie, Universität zu Köln, Zülpicher Straße 49b, 50674 Köln, Germany
[2]Institut für Geologie, Mineralogie und Geophysik Ruhr-Universität Bochum, 44780 Bochum, Germany

(*Received July* 11, 2003; *accepted in revised form February* 27, 2004)

Abstract—Diffusion couple experiments were carried out with San Carlos olivine (Fo_{90}) and NiFe alloys (Ni_{100}, $Ni_{97}Fe_3$, $Ni_{90}Fe_{10}$) or other olivine compositions (Fo_{100}, Fo_{25}) in order to determine the dependence on temperature, oxygen fugacity, composition and crystallographic orientation of Ni diffusion coefficient (D_{Ni}) in olivine. Experiments at 1 atmosphere total pressure cover a temperature range of 900–1445°C with run durations from 48 to 2155 h at different oxygen fugacities. In an Arrhenius plot the best fit for all data for Fo_{90} yields an activation energy (E_D) of 220 ± 14 kJ/mol and an fO_2 dependence of $(1/4.25) \cdot \Delta \log fO_2 = \Delta \log D_{Ni}$. The relationship between diffusion coefficients along different crystallographic axes at 1200°C is given by $D_{[001]} \approx 6 \cdot D_{[100]} \approx 6 \cdot D_{[010]}$. D_{Ni} depends strongly on the major element (i.e. Fe/Mg) composition of olivine and decreases by about 1 order of magnitude as the olivine composition changes from Fo_{35} to Fo_{90}. Thus, experimental investigations in Fe-free systems cannot be applied to natural samples. For calculation of residence times or cooling rates the present Ni data yield shorter timescales compared to those obtained using diffusion data published until now.

In addition to Ni diffusion coefficients, Fe-Mg, Mn and Ca diffusion data were obtained from some of the same diffusion couples (Fo_{90}-Fo_{100}). It is found that the activation energies, $E_D[Ni] \cong E_D[Fe\text{-}Mg] \cong E_D[Mn] \leq E_D[Ca]$. All diffusion coefficients are strongly dependent on the major element composition of olivine.

1. INTRODUCTION

Diffusion coefficients in combination with element partitioning data may be used to constrain thermal histories of a variety of terrestrial and extra terrestrial rocks. Geospeedometric techniques can be used to obtain cooling rates (e.g., Lasaga, 1983) or the durations of entire thermal events as well as just the heating or cooling parts of the thermal cycle (e.g., Chakraborty and Ganguly, 1991). The exchange of Ni and Fe between olivine and metal is strongly temperature dependent (e.g., see Petry, 1999) and is thus ideally suited for the determination of thermal histories of metal bearing silicate meteorites, that constitute the majority among all meteorite types. To develop this tool, it is necessary to quantify (a) the partitioning of Ni between metal and olivine and (b) the diffusion rates of Ni in olivine. We have carried out an experimental study to address both issues (Petry, 1999). In this paper we report the results of the measurement of diffusion coefficients in olivine. The results on element partitioning will be discussed elsewhere.

Nickel, as a strongly compatible element, becomes concentrated in olivine through terrestrial magmatic processes. Therefore, modelling the compositional zoning of Ni in terrestrial olivine samples has been used to constrain thermal histories of volcanic and plutonic processes (e.g., Nakamura, 1995). Detailed measurements of Ni diffusion rates in olivine can quantify and improve the understanding of such processes. Our experimental approach results in the simultaneous determination of diffusion rates of additional divalent cations in Fe-bearing olivine besides Ni (e.g., Fe-Mg, Mn and some limited information on Ca). This allows the verification of existing diffusion data and most importantly, allows study of subtle differences between the diffusion rates of various cations in olivines.

We have used olivine (Fo_{90})-metal (Ni_{100}, $Ni_{97}Fe_3$, $Ni_{90}Fe_{10}$) or olivine (Fo_{90})-olivine (Fo_{100}, Fo_{25}) single crystal diffusion couples to obtain Ni diffusion coefficients between 900 and 1445°C as a function of temperature, oxygen fugacity, composition and crystallographic orientation, all at a total pressure of 1 atm.

2. EXPERIMENTAL METHOD

2.1. Starting Material and Anneals

The experimental methods were similar to those of Chakraborty (1997) and details of crystals used, sample preparation, experimental setup and annealing procedures may be found there as well as in Petry (1999). All experiments were carried out using single crystals of olivine that were oriented using X-ray diffraction. A surface perpendicular to the direction in which diffusion rates were to be measured was then polished using diamond compounds, followed by a final step where a colloidal silica compound was used. For individual diffusion anneals, pieces ~2 mm on the side were sawed from the larger pieces using a fine diamond saw. Compositions of all starting materials used are given in Table 1.

Diffusion couples were held in a vertical gas mixing furnace under defined temperatures and oxygen fugacities (maintained by a flowing gas mixture of CO-CO_2) which were continuously monitored using Pt-Rh thermocouples and ZrO_2 sensors, respectively. Run conditions were chosen to be within the stability field of both partners of a diffusion couple.

Two experimental approaches were used to check consistency as well as to determine the dependency of diffusion rates on different variables. In the first approach, oriented single crystals of San Carlos olivine (Fo_{90}) and metal alloys of different compositions (Ni_{100},

* Author to whom correspondence should be addressed, at Wilhelmshöher Allee 289, 34131, Kassel, Germany (sumit.chakraborty@ruhr-universität-bochum.de).

Table 1. Composition of starting crystals and metal alloys.

(wt%)	Fo_{100}	~Fo_{90}	Fo_{25}
FeO	0.15	8.7–11.1	56.8
MgO	56.5	49.8–47.8	7.9
SiO_2	42.5	41.4–40.4	31.9
NiO	—	0.36	< d.l.
MnO	—	0.14	4.05
CaO	—	0.09	< d.l.
Total	99.15	~99.9	100.35
(atom%)*		(Ø)	*at 4 O
Fe	0.0030	0.1781	1.5191
Mg	1.9893	1.7970	0.3741
Si	1.0039	1.0063	1.0039
Ni		0.0071	
Mn		0.0029	0.1090
Ca		0.0024	

(atom%)	Ni_{100}	$Ni_{99.9}$	$Ni_{97}Fe_3$	$Ni_{90}Fe_{10}$
Ni	100	99.9	97.2	90.1
Fe	—		2.8	9.9
Mn	—	0.1	—	—

$Ni_{97}Fe_3$, $Ni_{90}Fe_{10}$) were pressed together using a spring loaded setup in an Al_2O_3 holder. The metal alloys were prepared by melting mixtures of metal filings of Ni and Fe in a reducing atmosphere; the composition and homogeneity were verified by electron microprobe analysis. Blocks of these alloys were then used as exchange partners for the olivines in the diffusion anneals. Run durations were up to 280 h, depending on temperature, to achieve concentration profiles 10–200 μm in length.

With an olivine-metal couple the effects of oxygen fugacity and composition on the Ni diffusion rate could not be separated. The content of Ni in olivine in equilibrium with Ni metal and the diffusion coefficient of Ni in olivine both increase with increasing fO_2. Figure 1 illustrates the difficulty. At a temperature of 1200°C, runs carried out at oxygen fugacities of 10^{-4}, 10^{-5} and 10^{-6} Pa show a decrease of Ni content at the interface from 10 wt% to 1.8 wt% NiO. Differences in retrieved diffusion coefficients from such profiles cannot be unequivocally attributed to either fO_2 or Ni content. Therefore, another alternative experimental approach was employed using olivine-olivine diffusion couples. These diffusion couples also allow a test for consistency of diffusion data and eliminate the possibility that convolution effects, resulting from fluorescence in the electron microprobe from the Ni-rich alloys (e.g., Ganguly et al., 1988; Dalton and Lane, 1996), substantially distort the results.

That convolution effects can be substantial for the measurement of a trace element next to a source containing the pure metal is illustrated in Figure 2). In this sample, annealed for only 15 min at 1200°C, a pseudo concentration profile of Ni extending up to 40 microns within the crystal can be measured. Subsequent measurements of diffusion coefficients indicate that there cannot be any diffusion profile induced within such a short time (expected length of profile is less than a micron) and all of the effect seen in this sample is an artefact. In addition, no concentration profile of Fe is observed within the olivine although a large concentration gradient exists at the interface between Fe-free metal and Fe-bearing olivine. Unwittingly fitting the Ni profile to retrieve a diffusion coefficient yields a number that is three orders of magnitude faster than the real diffusion coefficient. This highlights the potential perils resulting from convolution effects, particularly when the diffusion coefficients of trace elements are being measured. For olivine-metal diffusion couples from which data are reported in this study care was taken to ensure that the concentration of Ni measured in olivine at the interface was much higher than that due to convolution alone (0.6 wt% NiO) so that the profile shapes are not distorted by this effect.

To overcome these difficulties, two kinds of olivine-olivine diffusion couples were used. Fo_{90}-Fo_{100} couples were annealed up to 2159 h to determine the oxygen fugacity dependence of the Ni diffusion coefficients. Fo_{90}-Fo_{25} couples were used to characterize the dependence of Ni diffusion rates on olivine composition (major elements i.e., Fo/Fa ratio). The Fo_{100} and Fo_{25} crystals used here come from the same stock that was used by Chakraborty (1997) and detailed descriptions of the source and chemistry of these crystals, including trace element concentrations, are provided in that work.

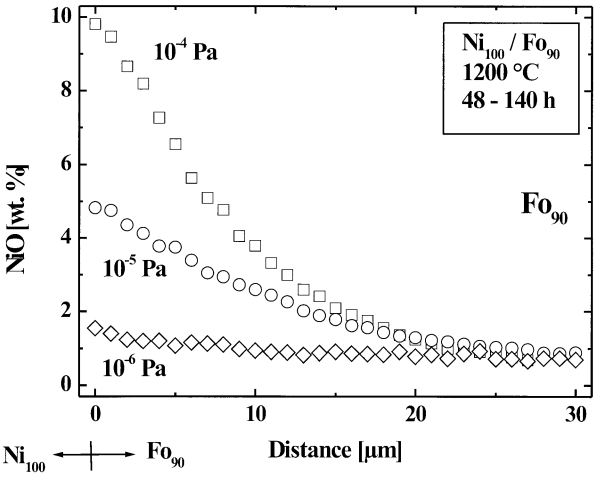

Fig. 1. Ni diffusion profiles in olivine of Ni_{100}-Fo_{90} couples at 1200°C and different oxygen fugacities showing increasing NiO concentration at the interface with increasing oxygen fugacity of the experimental anneal.

As the chemical potential of SiO_2 in the surrounding medium has the potential to affect stability as well as point defect chemistry of olivine, it is important to consider the role of this variable in the present set of experiments. The chemical potential of SiO_2 was not explicitly controlled in our experiments. The olivine-olivine diffusion couples of this study are identical to those used by Meissner et al. (1998) and Meissner (2000). In her detailed HRTEM study, Meissner (2000) found no evidence of formation of new phases or decomposition of olivine. We have not seen any evidence of formation of any new phases at least on the resolution of a SEM in the metal-olivine couples as well. Hence, the stability of olivine is not a concern for the conditions covered in our experiments. The influence of the ambient chemical potential of SiO_2

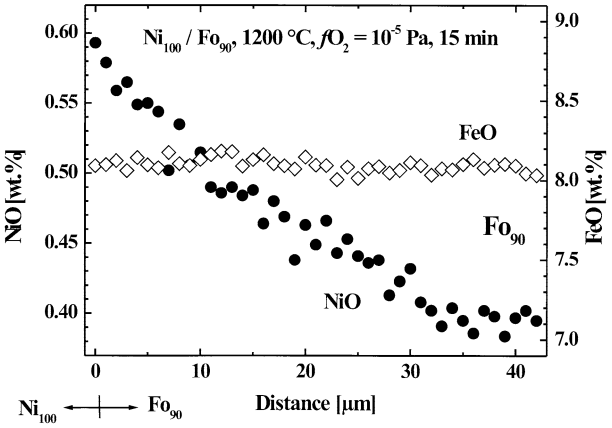

Fig. 2. Convolution effect in the measurement of Ni in olivine (trace element) against a metallic alloy of Ni using the electron microprobe. The concentration gradient observed here is an artifact, see text for details of the sample and beam conditions during analysis in the microprobe.

Table 2. Compilation of all Ni diffusion coefficients (D_{Ni}) from olivine-metal and olivine-olivine couples. Diffusion coefficient presented for each run is the mean value obtained from fitting at least two and up to five concentration profiles measured on a given sample.

Sample	Diffusion couple	Temp. (°C)	log fO_2 (Pa)	Run duration (h)	D_{Ni} (m^2/s)	log D_{Ni} (m^2/s)
Ni 74	Fo_{90}-Fo_{100}	902	−9.92	2155.5	$1.0 \cdot 10^{-19}$	−19.00
Ni 64	Fo_{90}-Fo_{100}	1003	−6.10	670.45	$5.3 \cdot 10^{-18}$	−17.28
Ni 10	Ni_{100}-Fo_{90}	1005	−5.96	287.75	$7.6 \cdot 10^{-18}$	−17.12
Ni 67	Fo_{90}-Fo_{100}	1004	−7.04	334	$3.5 \cdot 10^{-18}$	−17.46
Ni 17	Ni_{100}-Fo_{90}	1100	−4.99	161	$4.7 \cdot 10^{-17}$	−16.33
Ni 26	$Ni_{97}Fe_3$-Fo_{90}	1100	−4.93	279.6	$3.9 \cdot 10^{-17}$	−16.41
Ni 29	Ni_{100}-Fo_{90}	1101	−5.07	106.33	$3.3 \cdot 10^{-17}$	−16.48
Ni 56	Fo_{90}-Fo_{100}	1102	−5.94	280.4	$3.2 \cdot 10^{-17}$	−16.49
Ni 9	Ni_{100}-Fo_{90}	1101	−6.05	159.25	$2.1 \cdot 10^{-17}$	−16.68
Ni 19	$Ni_{90}Fe_{10}$-Fo_{90}	1104	−5.99	165.75	$2.8 \cdot 10^{-17}$	−16.55
Ni 75	Fo_{90}-Fo_{100}	1102	−7.05	577	$7.8 \cdot 10^{-18}$	−17.11
Ni 16	Ni_{100}-Fo_{90}	1100	−6.97	161	$1.8 \cdot 10^{-17}$	−16.74
Ni 61	Fo_{90}-Fo_{100}	1104	−7.92	168.1	$6.2 \cdot 10^{-18}$	−17.21
Ni 18	Ni_{100}-Fo_{90}	1102	−7.98	165.25	$1.5 \cdot 10^{-17}$	−16.82
Ni 69	Fo_{90}-Fo_{100}	1154	−5.00	430	$7.6 \cdot 10^{-17}$	−16.12
Ni 77	Fo_{90}-Fo_{100}	1151	−7.11	573.75	$1.5 \cdot 10^{-17}$	−16.82
Ni 68	Fo_{90}-Fo_{100}	1154	−8.07	334	$1.3 \cdot 10^{-17}$	−16.89
Ni 58	Fo_{90}-Fo_{100}	1202	−4.00	259.83	$2.7 \cdot 10^{-16}$	−15.57
Ni 14	$Ni_{99.9}$-Fo_{90}	1203	−4.02	140	$2.3 \cdot 10^{-16}$	−15.64
Ni 30	$Ni_{99.9}$-Fo_{90}	1203	−5.05	72	$1.5 \cdot 10^{-16}$	−15.82
Ni 6	$Ni_{99.9}$-Fo_{90}	1203	−6.02	48.25	$8.1 \cdot 10^{-17}$	−16.09
Ni 4	$Ni_{99.9}$-Fo_{90}	1205	−5.89	184.33	$1.6 \cdot 10^{-16}$	−15.80
Ni 8	Ni_{100}-Fo_{90}	1252	−5.86	101	$1.6 \cdot 10^{-16}$	−15.80
Ni 78	Fo_{90}-Fo_{100}	1248	−6.95	222.75	$5.7 \cdot 10^{-17}$	−16.24
Ni 57	Fo_{90}-Fo_{100}	1303	−3.99	94.17	$1.5 \cdot 10^{-15}$	−14.82
Ni 3	Ni_{100}-Fo_{90}	1304	−3.86	161.33	$6.6 \cdot 10^{-16}$	−15.18
Ni 2	$Ni_{99.9}$-Fo_{90}	1303	−3.85	165.5	$1.3 \cdot 10^{-15}$	−14.89
Ni 21	$Ni_{90}Fe_{10}$-Fo_{90}	1305	−4.03	72	$6.8 \cdot 10^{-16}$	−15.17
Ni 20	$Ni_{90}Fe_{10}$-Fo_{90}	1302	−4.06	183	$6.1 \cdot 10^{-16}$	−15.21
Ni 23	$Ni_{90}Fe_{10}$-Fo_{90}	1298	−4.10	87	$8.3 \cdot 10^{-16}$	−15.08
Ni 59	Fo_{90}-Fo_{100}	1304	−5.89	245	$3.5 \cdot 10^{-15}$	−14.46
Ni 5	$Ni_{99.9}$-Fo_{90}	1300	−5.91	48.25	$3.1 \cdot 10^{-16}$	−15.51
Ni 52	Fo_{90}-Fo_{100}	1402	−3.86	231.16	$1.6 \cdot 10^{-15}$	−14.80
Ni 72	Fo_{90}-Fo_{100}	1403	−4.95	71	$1.3 \cdot 10^{-15}$	−14.89
Ni 55	Fo_{90}-Fo_{100}	1403	−4.94	280.42	$1.1 \cdot 10^{-15}$	−14.96
Ni 70	Fo_{90}-Fo_{100}	1403	−5.88	92.5	$9.5 \cdot 10^{-16}$	−15.02
Ni 37	$Ni_{97}Fe_3$-Fo_{90}	1403	−6.05	88	$5.3 \cdot 10^{-16}$	−15.28
Ni 36	$Ni_{97}Fe_3$-Fo_{90}	1445	−4.04	53	$2.5 \cdot 10^{-15}$	−14.60

on the transport rates of octahedral cations via its control of the point defect chemistry was not considered to be critical for a number of reasons. First, existing models (e.g., Stocker, 1978) of point defects in olivine as well as experimental studies (e.g., Barkmann and Cemic, 1996) indicate that vacancy concentrations in the octahedral sites are weakly dependent on this variable (for a system closed to net cation gain or loss) and the resulting effect on diffusion rates of cations in these sites would be below the resolution of the methods employed in this study. Second, in an earlier study on Mg tracer diffusion in olivines Chakraborty et al. (1994) did not find any measurable effect of this variable on diffusion rates. Finally, a posteriori, Ni diffusion coefficients obtained using a number of different crystals and experimental methods (diffusion couple, method of fitting concentration profiles etc.) are found to be consistent and reproducible once the effects of temperature, composition and oxygen fugacity are accounted for (all experiments were at the same total pressure). This suggests that the dominant variables controlling Ni diffusivity have been controlled in our experiments.

2.2. Measurement of Concentration Profiles

The concentration profiles were measured on polished surfaces of samples from all anneals along lines perpendicular to the interface using an electron microprobe. The step as well as beam size (diameter measured on fluorescent SnO_2) was typically 1 μm and counting times were 120 s on peak, using a focussed beam at operating conditions of 20 kV and 20 nA on a Faraday cage. A number of synthetic and natural silicate and metal standards were used for calibrations, and the measurements were further cross calibrated using measurements at different laboratories (e.g., most measurements in Cologne using a Cameca Camebax vs. some in Muenster using a JEOL 8600). Details of these calibration tests may be found in Petry (1999).

Concentrations of cations in olivines were normalized from 0 to 1 taking into account the total number of all octahedral cations (Fe, Mg, Ni, Ca, Mn) for all subsequent calculations. Diffusion coefficients were obtained from different runs as well as from different profiles in a single run. In addition, element mapping was carried out from diverse runs to verify that the shape of the diffusion front is parallel to the interface (i.e., enhanced diffusion along linear or planar defects, cracks etc. did not affect the results). Results from all runs are tabulated in Tables 2–4 including the composition of the diffusion couple, experimental conditions and diffusion coefficients retrieved.

2.3. Fitting the Concentration Profiles to Retrieve Diffusion Coefficients

Depending on the nature of the experiment, one of three different strategies was adopted to retrieve diffusion coefficients from measured concentration profiles. For the olivine-metal diffusion couples, where the concentration at the metal-olivine interface is held constant, the diffusion coefficient is independent of Ni concentration and the metal acts as an infinite reservoir. In this case, the solution to the diffusion equation is

Table 3. Ni, Fe-Mg, Mn, and Ca diffusion coefficients from all olivine-olivine experiments.

Sample	Temp. (°C)	log fO_2 (Pa)	log D_{Ni} (m^2/s)	log D_{FeMg} (m^2/s)	log D_{Mn} (m^2/s)	log D_{Ca} (m^2/s)
Ni 74	902	−9.92	−19.00	−18.83		
Ni 64	1003	−6.10	−17.28	−16.95		
Ni 67	1004	−7.04	−17.46	−17.42	−17.25	−18.66
Ni 56	1102	−5.94	−16.49	−16.37	−16.25	
Ni 75	1102	−7.05	−17.11	−16.94	−17.34	
Ni 61	1104	−7.92	−17.21	−17.31	−17.38	
Ni 69	1154	−5.00	−16.12			
Ni 77	1151	−7.11	−16.82	−16.57		
Ni 68	1154	−8.07	−16.89	−16.73	−16.79	
Ni 58	1202	−4.00	−15.57	−15.58	−15.69	
Ni 78	1248	−6.95	−16.24	−16.15		
Ni 57	1303	−3.99	−14.82	−14.86	−14.98	−15.53
Ni 59	1304	−5.89	−15.46	−15.27	−15.28	
Ni 52	1402	−3.86	−14.80	−14.65	−14.91	
Ni 72	1403	−4.95	−14.89	−14.76	−14.98	
Ni 55	1403	−4.94	−14.96	−14.81	−15.04	
Ni 70	1403	−5.88	−15.02	−14.75	−14.82	−15.28

$$\frac{C_x - C_{min}}{C_{interf} - C_{min}} = \mathrm{erf}\left[\frac{x}{2 \cdot \sqrt{D \cdot t}}\right] \quad (1)$$

where C_x is the concentration at distance x from the interface, C_{min} is the background concentration in the olivine, C_{interf} is the instantaneously imposed concentration at the metal-olivine interface, D is the diffusion coefficient and t is the annealing time. The assumption that Ni diffusion rate is independent of Ni-content was found to be justified a posteriori for the range of compositions studied in this work. A measured concentration profile and fit according to (1) is illustrated in Figure 3a.

For the Fo_{90}-Fo_{100} diffusion couples, the profiles were symmetric about the interface (Figs. 3b,c) and consequently, a solution to the diffusion equation for two infinite media in contact at the interface, with diffusion coefficient independent of concentration, was adequate:

$$\frac{C_x - C_{min}}{C_{max} - C_{min}} = \frac{1}{2} \cdot \mathrm{erfc}\left[\frac{x - x_o}{2 \cdot \sqrt{D \cdot t}}\right] \quad (2)$$

Here, x_o is the position of the interface. The constant D fit works in this case because the concentration dependence of Ni diffusion coefficients for a <10 mol.% change in fayalite content in the diffusion zone is negligible within the resolution of measurements. Eqns. 1 and 2 can either be fitted directly by nonlinear regression to the concentration profiles or a linear fit to an inverse error function plot can be made. Both approaches were tried and yield practically the same results; the data presented below are from the direct, nonlinear fits.

Table 4. Ni diffusion coefficients as a function of olivine composition from Fo_{90}-Fo_{25} diffusion couples.

	Log [D_{Ni} (m^2/s)]	
X_{Fe}	Ni 45 1100°C 10^{-7} Pa 257 h	Ni 73 1150°C 10^{-7} Pa 455 h
0.10	−16.37	−16.67
0.15	−16.28	−16.63
0.20	−16.28	−16.58
0.25	−16.08	−16.52
0.30	−15.99	−16.47
0.35	−15.88	−16.40
0.40	−15.79	−15.35
0.45	−15.68	−16.26
0.50	−15.55	−16.17
0.55	−15.47	−16.05
0.60	−15.35	−15.95
0.65	−15.23	−15.80
0.70	−15.09	−15.65

For Fo_{90}-Fo_{25} couples, the concentration dependence of Ni diffusion coefficients on fayalite content cannot be ignored, as seen from the strong asymmetry of the profile shapes (Figs. 3d,e), and diffusion coefficients were calculated at every composition, C*, using a Boltzmann-Matano analysis,

$$D_{C^*} = -\frac{1}{2 \cdot t} \cdot \left|\frac{dx}{dc}\right|^{C^*} \cdot \int_{C_L}^{C^*} x\,dc \quad (3)$$

where t is the run duration, x a distance coordinate and C_L the composition of the starting end-member. For applying this method to Ni profiles with only 3000 ppm Ni at the maximum, it was necessary to smooth the measured profiles to calculate slopes and areas required. Smoothing using the function

$$f(x) = \left[\frac{A_0}{1 + e^{(A_1 \cdot (x - A_2))^{A_3}}}\right] + A_4 \quad (4)$$

where $A_0 \ldots A_4$ are fit parameters, was found to work well in describing the measured profile shapes.

2.4. Chemical or Self Diffusion Coefficients?

In all of the experiments described above, the rate of diffusion of Ni in the presence of a chemical concentration gradient i.e., chemical diffusion coefficients are measured. Even more strictly, what is measured is a multicomponent exchange diffusion rate of Ni-Fe-Mg (± Mn ± Ca) and the corresponding multicomponent formulations should be used to model the concentration profiles. Such multicomponent effects are indeed observed in some olivine-metal diffusion couples, where in addition to the main Ni-Fe exchange taking place, weak uphill diffusion of Mg within the olivine is observed (for Mg the olivine-metal interface is practically an insulating boundary) in response to the concentration gradients of Ni and Fe. However, for a dilute constituent such as Ni the chemical diffusion coefficients become practically identical to the self or tracer diffusion coefficients (e.g., see Lasaga, 1979; Allnatt and Lidiard, 1993) *at the same composition*. Ni contents in olivines are within trace element levels in all olivine–olivine diffusion couples and most olivine–metal diffusion couples and therefore the diffusion coefficients we retrieve using the above formalisms are all essentially the self- or tracer diffusion coefficients of Ni in olivines of a given major element composition. Here we club self- or tracer diffusion coefficients together to contrast them with chemical- or interdiffusion coefficients, ignoring the much smaller differences between these quantities them-

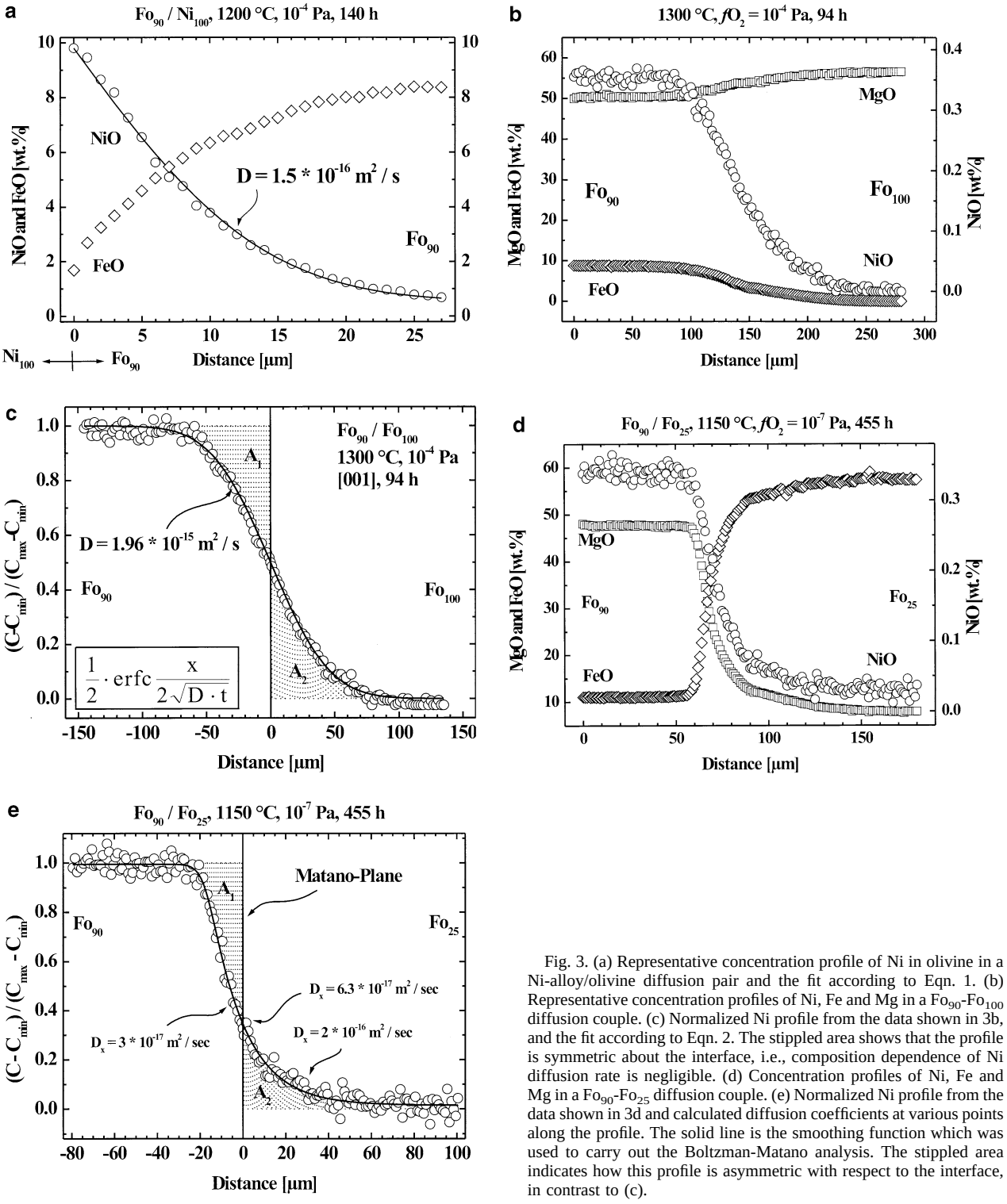

Fig. 3. (a) Representative concentration profile of Ni in olivine in a Ni-alloy/olivine diffusion pair and the fit according to Eqn. 1. (b) Representative concentration profiles of Ni, Fe and Mg in a Fo_{90}-Fo_{100} diffusion couple. (c) Normalized Ni profile from the data shown in 3b, and the fit according to Eqn. 2. The stippled area shows that the profile is symmetric about the interface, i.e., composition dependence of Ni diffusion rate is negligible. (d) Concentration profiles of Ni, Fe and Mg in a Fo_{90}-Fo_{25} diffusion couple. (e) Normalized Ni profile from the data shown in 3d and calculated diffusion coefficients at various points along the profile. The solid line is the smoothing function which was used to carry out the Boltzman-Matano analysis. The stippled area indicates how this profile is asymmetric with respect to the interface, in contrast to (c).

selves due to the correlation coefficient. The approximation resulting from low concentrations is clearly not valid for some olivine–metal couples where Ni concentrations in olivine of up to 10% were attained, as noted above. This is one more reason for using the olivine-olivine couples to filter out any possible effects resulting from the dependence of Ni diffusion rates on the Ni content of olivine. However, a posteriori consistency of data from different kinds of diffusion couples (see below) indicate a fortuitous independence of Ni diffusion rates on Ni content, at least within the range encompassed in this study, such that the generalization that Ni self- or tracer diffusion coefficients are being measured extends even to these relatively Ni rich samples. This is possibly a consequence of the dominant role of Fe in controlling the point defect chemistry of olivines, as discussed below.

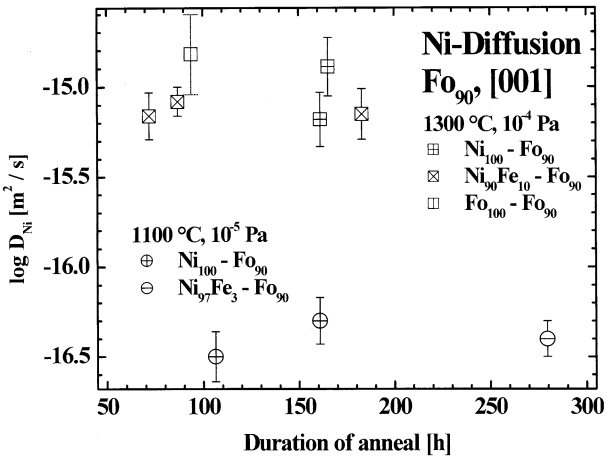

Fig. 4. Ni diffusion coefficients of different experimental runs at 1100 and 1300°C showing independence from run durations.

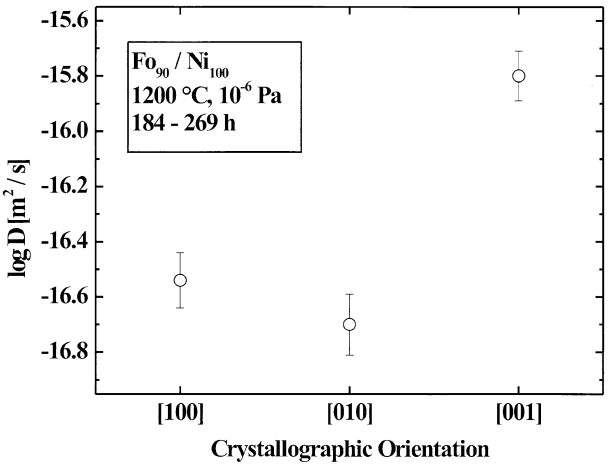

Fig. 5. Ni diffusion coefficients along different crystallographic orientations from Ni_{100}-Fo_{90} runs.

3. RESULTS AND DISCUSSION

All retrieved diffusion coefficients are presented in Tables 2–4. As an internal consistency check, data from runs at the same temperature and oxygen fugacity but using different couples and run durations were compared to see if diffusivities are solely defined by temperature, fO_2, major element composition, crystallographic orientation and pressure. Figure 4 is a plot of the Ni diffusion coefficients obtained from 6 different runs at 1300°C and 3 different runs at 1100°C. The Ni diffusion coefficients are the same within error and are independent of run duration and diffusion couple (and therefore, fitting method) used to obtain these. The propagation of the statistical error of analysis only results in an uncertainty of 20% or less for retrieved diffusion coefficients. This is clearly true for multiple profiles measured from the same sample; in most cases the results of fitting such profiles are identical. However, a true measure of the overall uncertainty in the diffusion coefficients resulting from various unquantifiable sources of errors is in the reproducibility of data from the different kinds of experiments and fitting methods. This uncertainty, as seen from the scatter of the mean values in Figure 4, is about a factor of two.

The dependence of Ni diffusion coefficients in olivine on crystallographic orientation is illustrated in Figure 5. Diffusion profiles in Fo_{90}-Ni_{100} couples were measured along [100], [010] and [001] for runs carried out at 1200°C and an fO_2 of 10^{-6} Pa. Diffusivities along the a- [100] and b-[010] axes are similar, whereas, the diffusion rate along the c-axis, [001], is six times greater at this temperature. To avoid long run durations, influence of all other parameters on Ni diffusion rates in olivine were determined in experiments where diffusion occurred along [001].

The least squares fit to all experimental data along [001] as a function of temperature (1000 to 1400 C) at a constant fO_2 of 10^{-6} Pa yield an activation energy (E_D) of 216 kJ/mol and a preexponential factor of $3.84 \cdot 10^{-9}$ m^2/s. (Fig. 6). While we have fitted the most extensive data set that we have at a particular fO_2, a plot of all Ni diffusion coefficients at different temperatures and fO_2 conditions (Fig. 7) indicates that diffusion rates of Ni increase with increasing fO_2 as well as T, and diffusion coefficients at different oxygen fugacities define subparallel lines on an Arrhenius diagram. In other words, there is no change of activation energy, and by implication, diffusion mechanism, over the entire range of T and fO_2 studied. Consequently, fits to all data yield an average E_D for all experiments of 220 kJ/mol and an fO_2 dependence exponent of 1/4.25.

The Ni diffusion coefficients as a function of the major element composition (=Fo content) of olivine are shown in Figure 8. Data from a Fo_{90}-Fo_{25} couple annealed at 1150°C, $fO_2 = 10^{-7}$ Pa show that D_{Ni} increases by an order of magnitude for an increase in Fe content of olivine from Fo_{90} to Fo_{25}. At Fo_{90}, we are able to compare D_{Ni} obtained from a completely different experiment—a Fo_{90}-Fo_{100} couple annealed at the same experimental conditions. The excellent agreement in D_{Ni} values demonstrates again the internal consistency of various experimental approaches. Furthermore, extrapolation of the D_{Ni} vs. Fayalite content trend to pure forsterite yields a value that is only slightly faster than the

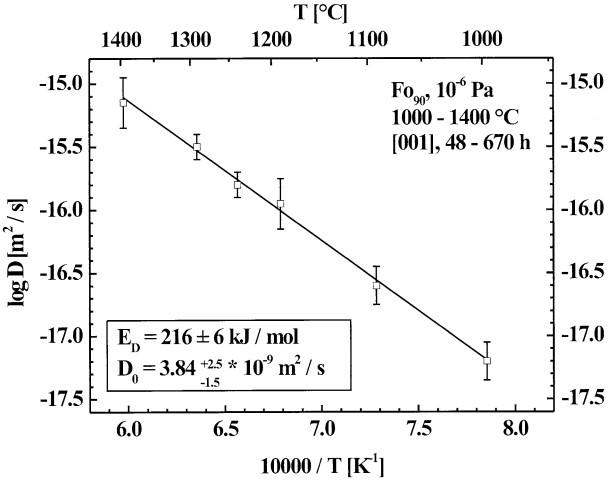

Fig. 6. Temperature dependence of Ni diffusion coefficient along [001] between 1000 and 1400°C at an oxygen fugacity of 10^{-6} Pa.

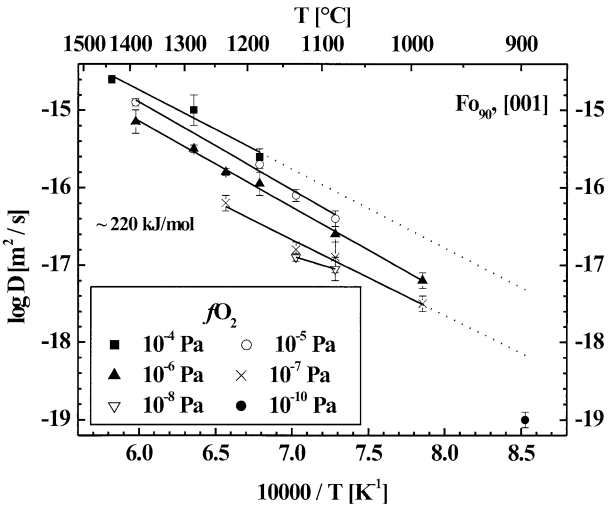

Fig. 7. Temperature (900–1145°C) and oxygen fugacity (10^{-4}–10^{-10} Pa) dependence of Ni diffusion coefficient in olivine. Experimental run durations were between 48 and 2155 h.

determinations of Morioka (1981), who used synthetic Mg_2SiO_4-Ni_2SiO_4 couples as starting end-members or Ito et al. (1999), who used doped NiO thin films on synthetic forsterite. However, the activation energy of ~400 kJ/mol obtained in these studies is substantially different from the 220 kJ/mol obtained in this work, so that at progressively lower temperatures, the discrepancy between these data sets will become larger. This discrepancy is, however, a physically meaningful one consistent with the fact that the presence of Fe makes the formation of vacancies easier and thereby reduces the activation energies for diffusion (see below as well as Chakraborty et al., 1994, and Chakraborty, 1997, for detailed discussions).

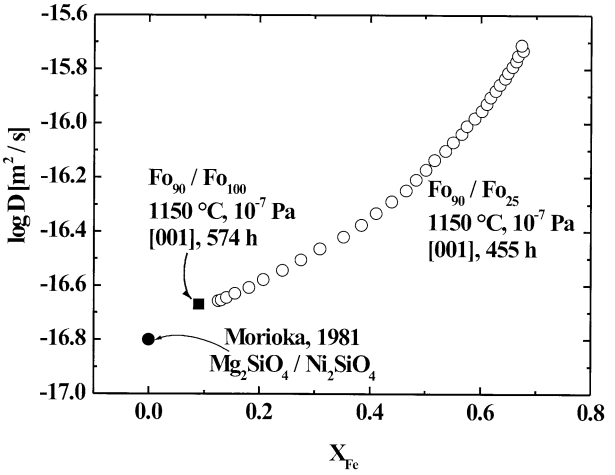

Fig. 8. Concentration dependence of the Ni diffusion coefficient on the Fe content of the olivine from an experiment carried out with a Fo_{90}-Fo_{25} diffusion couple. For comparison, data from a Fo_{90}-Fo_{100} run as well as the result from Morioka (1981) are shown. Error bars on individual determinations of diffusion coefficients are not larger than the symbol sizes. True errors are obtained from reproducibility of data obtained from different experiments and may be larger, such repeated experiments are not available in this case.

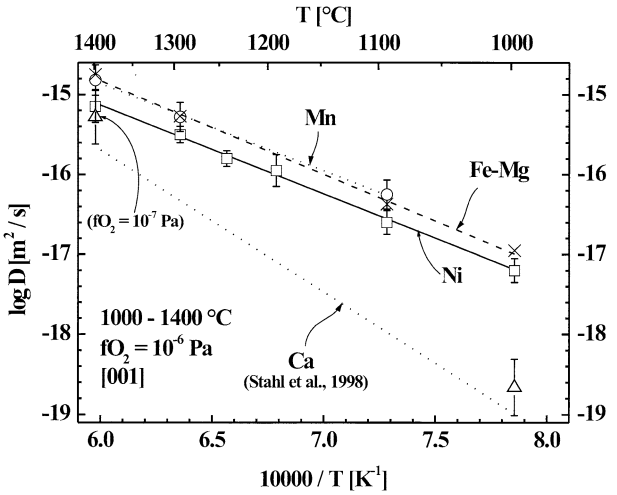

Fig. 9. Cation (Ni, Fe-Mg, Mn, Ca) diffusion coefficients in olivine between 1000 and 1400°C at an oxygen fugacity of 10^{-6} Pa. Cross-Mn, Circle-Fe-Mg, Squares-Ni and Triangles-Ca. Best fit lines are shown for Ni, Fe-Mg and Mn, whereas for Ca, the Arrhenius line from Stahl et al. (1998), which appears to be consistent with the data from this study, is shown to ease comparison of Ca data with the others.

Such differences in activation energies between Fe-free and Fe-bearing systems have been documented earlier for Mg diffusion in olivine (Chakraborty et al., 1994), diopside (Cherniak, 2001), spinel (Liermann and Ganguly, 2002) and (Mg,Fe) oxides (Bygden et al., 1997). The important implication of this experimental observation for the diffusion of a trace element such as Ni is a reinforcement of the observation already made by Chakraborty (1997) for major elements-diffusion coefficients and activation energies for any species measured or calculated in Fe-free systems cannot be used to model these in Fe-bearing natural systems.

Finally, the different forsterite contents as well as Mn and Ca concentrations in the starting olivines of the San Carlos (Fo_{90})–synthetic forsterite (Fo_{100}) couples allow simultaneous measurement of concentration profiles of all of these constituents and the determination of the relevant diffusion coefficients where the profiles were sufficiently free of noise. The data, reported in Table 3, are illustrated for comparison to Ni diffusion coefficients in Figure 9. The salient aspect of this comparison is that all of these cations, with the exception of Ca, diffuse at practically the same rates and with the same activation energies. In detail, Mn and Fe diffuse only marginally faster than Ni. From a practical standpoint, this is of immense significance because this observation indicates that (a) concentration profiles of all divalent cations that occupy octahedral M-sites, with the exception of Ca, can be modeled using the same diffusion coefficient, and (b) no kinetic fractionation of any of these elements from one another is to be expected due to differing diffusion rates in olivines.

This observation also provides us with key insights for understanding diffusion mechanisms. The relative independence of diffusion rates and activation energies from ionic size, as long as the ions can occupy the same crystallographic site (M1 in olivine), shows that some parameter related to the characteristic of this site, rather than the ions themselves, is the determining factor. Based on what is known about defects and

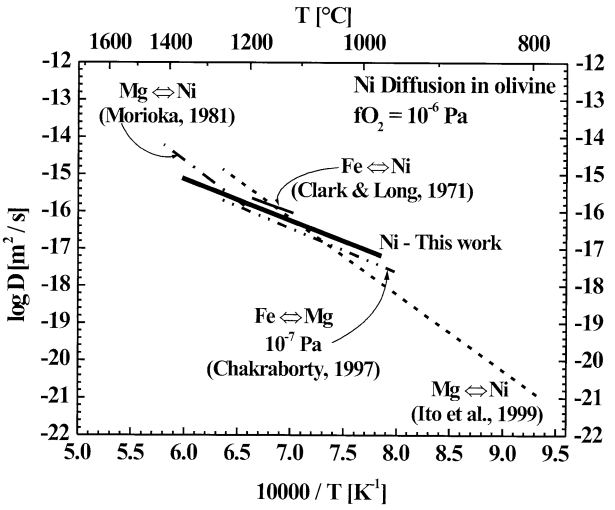

Fig. 10. Comparison of Ni diffusion data from this study with results from earlier work (Clark and Long, 1971; Morioka, 1981; Ito et al., 1999).

diffusion in olivines, it is quite apparent what these characteristics are: ease of vacancy formation and geometric proximity. In an olivine, it is energetically much more efficient to produce vacancies in the M1 site (e.g., Lasaga, 1980; Brodholt, 1997). For example, Lasaga (1980) finds that it is about ten orders of magnitude more likely to produce a vacancy in the M1 site compared to that in the M2 site at 1000°C. Vacancy formation becomes even easier in the presence of Fe, which supplies an energetically "cheap" dopant in the form of Fe^{3+}. Added to this, one has the geometric contiguity of the M1 sites; it is possible to produce a continuously connected path made up of only M1-M1 jumps along [001], as discussed by Brodholt (1997) in detail. This is all consistent with, and nicely explains, the in situ Mössbauer observations of Niemeier et al. (1996) that in an olivine crystal, M1-M1 jumps occur far more frequently than either M1-M2 or M2-M2 jumps. So, ions that are able to occupy the M1 sites in olivine all avail the same easy paths and the same vacancies (produced primarily by the presence of Fe^{3+} in the structure, at least in "dry" olivines, see, for example, Nakamura and Schmalzried, 1983) for diffusion, particularly along [001]. Therefore, it is no surprise that all of these ions have practically the same diffusion coefficients. In contrast Ca, which on account of its larger size is unable to occupy the M1 position and is restricted to M2, has a much slower diffusion rate and much higher activation energy of diffusion, because neither the easily created vacancies, nor the connected M1-M1 paths, are accessible to it.

4. DIFFUSION OF Fe-Mg, Mn AND Ca AND COMPARISON WITH PREVIOUS DATA

Plotting the new data at an fO_2 of 10^{-6} Pa (our most extensive set) in an Arrhenius diagram it can be seen (Fig. 10) that there is excellent agreement between our results and those from the earlier published study of Clark and Long (1971), where measurements were carried out over a restricted range of temperature (only 1150–1234°C). However, this agreement is somewhat fortuitous as Clark and Long (1971) did not control fO_2 because of the manner in which their experiment was set up. If we take data from some other fO_2 from our study for comparison, the agreement will not be as perfect, but it will remain rather good nonetheless, particularly when it is taken into account that the measurements of Clark and Long were very preliminary in nature; in fact, these were among the very first reports of diffusion coefficients in a silicate mineral of geological interest! Moreover, the diffusion anisotropy measured by us is practically identical to that measured by Clark and Long (1971).

Morioka (1981) studied Ni diffusion in an Fe-free system (Mg_2SiO_4-Ni_2SiO_4 couples) at higher temperatures (1250–1450°C) and obtained a much higher activation energy (414 kJ/mol). Subsequently, Ito et al. (1999) measured Ni diffusion rates in the same system using a very different set up of NiO thin films on forsterite single crystals. With this setup and using SIMS, they were able to measure diffusion rates over a large temperature range from 800 to 1300°C. They obtained very similar diffusion coefficients to those of Morioka (1981) and observed that a single activation energy describes diffusion over the entire temperature range i.e., there was no evidence of any change of mechanism as sometimes postulated. They also observed that Mg, Co and Ni diffusion rates and activation energies are very similar in these Fe-free systems. At the same time, these activation energies (~400 kJ/mol) are distinct (~220 kJ/mol) from those in the Fe-bearing systems, as seen above. Taken together, a consistent picture emerges from these data:

(i) the high and low activation energies obtained in different studies are not related to change of diffusion mechanisms from intrinsic to extrinsic in any given substance. Instead, it is related to the difference in the nature of the substances in which diffusion is measured, namely Fe-bearing and Fe-free olivines. This difference is related specifically to the special role of Fe in creating defects and does not indicate that variations in the concentrations of arbitrary trace elements would cause diffusion coefficients to vary widely. That diffusion coefficients remain reproducible, measurable quantitites once differences in Fe contents are accounted for has now been repeatedly demonstrated, e.g., in this study for various starting materials and Ni contents, for the Fe free systems in the studies of Ito et al. (1999) and Morioka (1981) (who used different sources for Ni-NiO vs. Ni_2SiO_4) as well as for Fe-Mg diffusion (Chakraborty, 1997; this study).

(ii) Activation energies for the different divalent cations that can occupy the M1 site (e.g., Fe, Mg, Mn, Ni, Co) are very similar in the Fe-bearing as well as in the Fe-free olivines, although between the two groups of materials there are large differences. This indicates that within each group diffusion occurs by one dominant mechanism, although the mechanism of diffusion is very different in Fe-free and Fe-bearing olivines. The fact that diffusion rates depend on chemical potentials (e.g., fO_2) indicates that diffusion occurs by an extrinsic mechanism (e.g., see Schmalzried, 1983). In addition, for Fe bearing olivines, the dependence of diffusion rates on Fe content but not on other arbitrary constituents shows that diffusion of all of these elements occurs by the kind of extrinsic mechanism defined by Chakraborty (1997) as transition metal extrinsic (TaMED). This mechanism incorporates aspects of both, the classical intrinsic (e.g., point defect concentrations are a func-

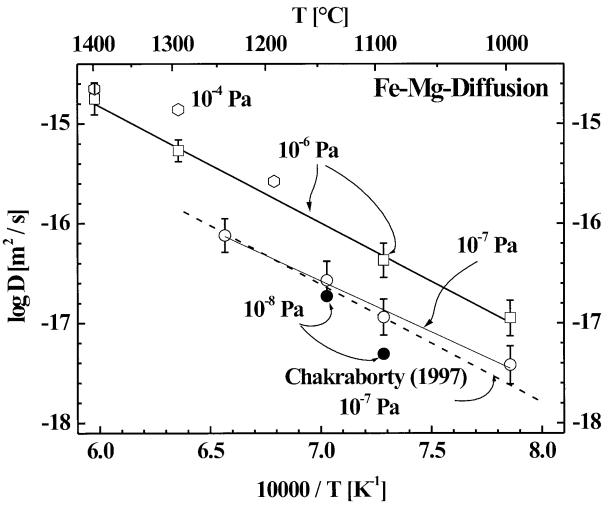

Fig. 11. Comparison of Fe-Mg diffusion data at different oxygen fugacity with the results from Chakraborty (1997) obtained at 10^{-7} Pa.

tion of temperature) as well as extrinsic (e.g., point defect concentrations are a function of some chemical potential i.e., dopant concentration) diffusion.

(iii) Because of the large differences in activation energies, diffusion rates in Fe-free olivines may be faster (at higher temperatures) or slower than in Fe-bearing olivines and the difference increases as one moves away from the crossover temperature (ca. 1250°C for Ni). Therefore, for applications to natural, Fe bearing olivines appropriate Arrhenius relationships for Fe bearing olivines should be used to avoid errors in the estimation of time scales, cooling rates, etc.

Our next extensive set of data is for Fe-Mg diffusion and the results are practically identical to those of Chakraborty (1997) for an $fO_2 = 10^{-7}$ Pa, as shown in Figure 11. However, our data at an fO_2 of 10^{-6} Pa indicate that the fO_2 dependence for Fe-Mg diffusion is also given by an exponent of 1/4.25 (i.e., $D_{Fe\text{-}Mg} \propto fO_2^{1/4.25}$), analogous to Ni, at the conditions under which these diffusion anneals were carried out. This is a slightly stronger dependence than the typically assumed $(fO_2)^{1/6}$, based on results from Buening and Buseck (1973) for example. However, in the absence of a silica buffer, this is consistent with the experimental observations and point defect model of Nakamura and Schmalzried (1983), as shown by Barkmann and Cemic (1996) who obtained an exponent of 1/4.5 for pure fayalite for these conditions. In detail, however, the data suggests that the fO_2 dependence of diffusion rates in olivine may be more complex. Although the overall variation of $D_{Fe\text{-}Mg}$ as a function of fO_2 is well described by a $fO_2^{1/4.25}$ dependence, over different ranges of fO_2 (Fig. 11) it seems that the fO_2 exponent may be variable from ~1/2 to 1/6. The resolution of the current dataset is not adequate to address such subtle effects; specific experiments to characterize this variation are currently in progress. In view of the excellent agreement of the $D_{Fe\text{-}Mg}$ from this study with the data of Chakraborty (1997) and the detailed discussion of various other data sets for Fe-Mg in that work, we refrain from comparing our results with any of these other studies.

Our data for Mn and Ca diffusion are illustrated in Figure 9; the latter were only weakly constrained (the profiles were substantially noisier). Both of these diffusion rates appear to be slower than those determined by Jurewicz and Watson (1988) by ~0.5–0.7 log units, which can be accounted for by the fact that the experiments of Jurewicz and Watson (1988) were carried out under more oxidizing conditions. The activation energy for Mn diffusion found in both studies are practically identical. The activation energy for Ca is poorly constrained from this study, but the rates appear to be consistent with those found by Stahl et al. (1998). Clearly, more studies specifically designed to measure Ca diffusion are necessary to get definitive rates and activation energies. The dependence of diffusion rates on oxygen fugacity found in this work is the same as that observed by Jurewicz and Watson (1988) for diffusion along [001].

An important consequence of the similarity of diffusion rates and activation energies of Ni, Mn, Fe-Mg (and Co, by inference from data in Fe-free systems) and the dissimilarity of Ca diffusion rates is that a compensation law is not a very meaningful description of the diffusion coefficients of divalent cations in olivine of a given composition.

5. SUMMARY

The primary contribution of this study is the determination of Ni diffusion rates in Fe-bearing olivines as a function of temperature (900–1445°C), composition (Fo_{25}-Fo_{100}), oxygen fugacity (10^{-4}–10^{-10} Pa) and crystallographic orientation. An activation energy of 220 ± 14 kJ/mol describes the diffusion of Ni in all olivines studied here and this activation energy remains constant over the entire temperature range. Ni diffusion rates increase by about an order of magnitude as Fe content of olivine increases from Fo_{90} to Fo_{25}. The dependence of diffusion rates on oxygen fugacity in the absence of a silica buffer is found to be given by $D \propto fO_2^{1/4.25}$ i.e., somewhat stronger than $D \propto fO_2^{1/6}$. At 1200°C, diffusion rates along [100] and [010] are similar to each other and are about a factor of 6 slower than along [001]. Diffusion of Ni in olivine appears to be by a transition metal extrinsic (TaMED) mechanism.

Simultaneous determination of diffusion rates of Fe-Mg interdiffusion and Mn and Ca diffusion demonstrate that Fe, Mg and Mn show practically the same diffusion behavior (e.g., activation energy, fO_2 dependence and hence, diffusion mechanism) as Ni described above. This is true in both Fe free as well as Fe bearing olivines, although the diffusion behavior in each of these groups of materials is very different. The similarities as well as differences can be explained and understood as part of the same internally consistent picture based on what is known about the crystal structure and point defect systematics and energetics of olivines. This same set of properties of olivines also explain why the behavior of Ca diffusion is so different, with higher activation energies and consequently much slower diffusion rates at most temperatures.

The strong similarity of Ni, Mn, Co (the latter observed directly only in Fe-free olivines) and Fe-Mg diffusion rates indicates that a single diffusion coefficient will suffice to model the diffusion behavior of these elements in natural samples. Note that this does not imply that all of these elements will always diffuse to the same extent (i.e., same number of atoms exchange places) in any given condition; whether they do so will depend on the respective concentration gradients and

boundary conditions for the flux of each individual cation. The strong dissimilarity of diffusion behavior between Fe-free and Fe-bearing systems indicates that using data from Fe-free systems to model compositional evolution in Fe-bearing natural olivines will yield grossly incorrect results. As many earlier models of Ni transport in natural olivines have used the results of Morioka (1981) from a Fe-free system (e.g., Nakamura, 1995), the results from these studies will need to be revised.

Acknowledgments—We would like to thank the Deutsche Forschungsgemeinschaft (DFG) for generous funding to support this work and the entire staff of the mechanical, sample preparation and electronic workshop at the University of Cologne for their help in maintaining the laboratory. This work constitutes part of the doctoral dissertation of C.P. at the University of Cologne. We thank R. Dohmen, F. Costa and L. Coogan for their critical comments on an earlier version of the manuscript. Constructive comments from D. Cherniak, the associate editor F. Ryerson and two anonymous reviewers helped improve the manuscript.

Associate editor: F. J. Ryerson

REFERENCES

Allnatt A. R. and Lidiard A. B. (1993) *Atomic Transport in Solids*. Cambridge University Press.

Barkmann T. and Cemic L. (1996) Impedance spectroscopy and defect chemistry of fayalite. *Phys. Chem. Minerals* 23, 186–192.

Brodholt J. (1997) Ab initio calculations on point defects in forsterite (Mg_2SiO_4) and implications for diffusion and creep. *Am. Mineral*. 82, 1049–1053.

Buening D. K. and Buseck P. R. (1973) Fe-Mg lattice diffusion in olivine. *J. Geophys. Res*. 78, 6852–6862.

Bygden J., Jakobsson A., Sichen D., and Seetharaman S. (1997) Interdiffusion studies in the system MgO-FeO. Z. *Metallkd*. 88, 433–437.

Chakraborty S. (1997) Rates and mechanism of Fe-Mg interdiffusion in olivine at 980–1300°C. *J. Geophys. Res*. 102, 12317–12331.

Chakraborty S. and Ganguly J. (1991) Compositional zoning and cation diffusion in garnets. In *Diffusion, Atomic Ordering, and Mass Transport* (ed. S. K. Saxena), pp. 120–175. Advances in Physical Geochemistry 8. Springer.

Chakraborty S., Farver J. R., Yund R. A., and Rubie D. C. (1994) Mg tracer diffusion in synthetic forsterite and San Carlos olivine as a function of P, T and fO_2. *Phys. Chem. Minerals* 21(8), 489–500.

Cherniak D. J. (2001) Pb diffusion in Cr diopside, augite, and enstatite, and consideration of the dependence of cation diffusion in pyroxene on oxygen fugacity. *Chem. Geol*. 177, 381–397.

Clark A. M. and Long J. V. P. (1971) The anisotropic diffusion of nickel in olivine. In *Diffusion Processes* (eds. J. N. Sherwood, A. V. Chadwick, W. M. Muir, and F. L. Swinton), pp. 511–521. Gordon and Breach.

Dalton J. A. and Lane S. J. (1996) Electron microprobe analysis of Ca in olivine close to grain boundaries: The problem of secondary X-ray fluorescence. *Am. Mineral*. 81, 194–201.

Ganguly J., Bhattacharya R. N., and Chakraborty S. (1988) Convolution effects in the determination of compositional profiles and diffusion coefficients by microprobe step scan. *Am. Mineral*. 73, 901–909.

Ito M., Yurimoto M., Morioka M., and Nagasawa H. (1999) Co^{2+} and Ni^{2+} diffusion in olivine determined by secondary ion mass spectrometry. *Phys. Chem. Mineral*. 26, 425–431.

Jurewicz A. J. G. and Watson E. B. (1988) Cation in olivine, Part 1: Calcium partitioning and calcium-magnesium distribution between olivines and coexisting melts, with petrologic applications. *Contrib. Mineral. Petrol*. 99, 176–185.

Lasaga A. C. (1979) Multicomponent exchange and diffusion in silicates. *Geochim. Cosmochim. Acta* 43, 455–469.

Lasaga A. C. (1980) Defect calculation in silicates: Olivine. *Am. Mineral*. 65, 1237–1248.

Lasaga A. C. (1983) Geospeedometry: An extension of geothermometry. In *Kinetics and Equilibrium in Mineral Reactions* (ed. S. K. Saxena), pp. 81–114. Advances in Physical Geochemistry 3. Springer.

Liermann H. P. and Ganguly J. (2002) Diffusion kinetics of Fe^{2+} and Mg in aluminous spinel: Experimental determination and applications. *Geochim. Cosmochim. Acta* 66, 2903–2913.

Meissner E. (2000) Messung von kurzen Konzentrationsprofilen mit Hilfe der analytischen Transmisssionselektronenmikroskopie (TEM-EDX) am Beispiel der Bestimmung von Diffusionskoeffizienten für die Fe-Mg Interdiffusion in Olivin. Dissertation, Universität Bayreuth.

Meissner E., Sharp T. G., and Chakraborty S. (1998) Quantitative measurement of short compositional profiles using analytical transmission electron microscopy (ATEM). *Amer. Mineral*. 83, 546–552.

Morioka M. (1981) Cation diffusion in olivine—II. Ni-Mg, Mn-Mg, Mg and Ca. *Geochim. Cosmochim. Acta* 45, 1573–1580.

Nakamura M. (1995) Residence time and crystallization history of nickeliferous olivine phenocrysts from the northern Yatsugatake volcanoes, Central Japan: Application of a growth and diffusion model in the system Mg-Fe-Ni. *J. Volcanol. Geotherm. Res*. 66, 81–100.

Nakamura A. and Schmalzried H. (1983). On the nonstoichiometry and point defects of olivine. *Phys. Chem. Mineral*. 10, 27–37.

Niemeier D., Chakraborty S., and Becker K. D. (1996) A high-temperature Mössbauer study of the directional geometry of diffusion in fayalite, Fe_2SiO_4. *Phys. Chem. Minerals*. 23, 284.

Petry C. (1999) *Experiment zur Ni-Diffusion in Olivin, Kalibration des Ni-Fe/Metall-Olivin—Austauschthermometers und deren Anwendung in der Kosmochemie*. Tectum Verlag.

Schmalzried H. (1983) Thermodynamics of compounds with narrow ranges of nonstoichiometry. *Ber. Bunsenges. Phys. Chem*. 87, 726–733.

Stahl S., Hain A., Chakraborty S., Laqua W., and Palme H. (1998) Tracer diffusion of ^{42}Ca in olivine as a function of composition and pO_2 between 800 and 1500°C. *Eos* 79, S370.

Stocker R. L. (1978) Influence of oxygen pressure on defect concentrations in olivine with a fixed cationic ratio. *Phys. Earth Planet. Interiors* 17, 118–129.